Hindawi Publishing Corporation
International Journal of Distributed Sensor Networks
Volume 2015, Article ID 138328, 12 pages
http://dx.doi.org/10.1155/2015/138328

Research Article

Energy-Efficient Layered Video Multicast over OFDM-Based Cognitive Radio Systems

Wenjun Xu, Shengyu Li, Yue Xu, Zhiyong Feng, and Jiaru Lin

Key Lab of Universal Wireless Communications, Ministry of Education, Beijing University of Posts and Telecommunications, Beijing 100876, China

Correspondence should be addressed to Wenjun Xu; wjxu@bupt.edu.cn

Received 10 July 2015; Accepted 17 September 2015

Academic Editor: Miao Pan

An energy-efficient layered video multicast (LVM) scheme for "*bandwidth-hungry*" video services is studied in OFDM-based cognitive radio (CR) systems, where the video data is encoded into a base layer and several enhancement layers with the former intended for all subscribers to guarantee the basic quality of reconstructed video and the latter aiming at the quality improvement for the promising users with good channel conditions. Moreover, in order to balance user experience maximization and power consumption minimization, a novel performance metric *energy utility* (EU) is proposed to measure the sum achieved quality of reconstructed video at all subscribers when unit transmit power is consumed. Our objective is to maximize the system EU by jointly optimizing the intersession/interlayer subcarrier assignment and subsequent power allocation. For this purpose, we first perform subcarrier assignment for base layer and enhancement layers using greedy algorithm and then present an optimal power allocation algorithm to maximize the achievable EU using fractional programming. Simulation results show that the proposed algorithms can adaptively capture the state variations of licensed spectrum and dynamically adjust the video transmission to exploit the scarce spectrum and energy resources adequately. Meanwhile, the system EU obtained in our algorithms is greatly improved over traditional spectrum efficiency (SE) and energy efficiency (EE) optimization models.

1. Introduction

Recently, the fifth generation (5G) mobile wireless system has been under heated discussion [1, 2]. It is reported that the wireless traffic volume will increase by 1000-fold over the next decade [3], and hence there is an urgent need to design novel spectrum-efficient transmission paradigms. Cognitive radio (CR) [4] is one of the best technologies to improve the spectrum efficiency (SE) and has attracted many researchers' attention. The basic idea of CR is to bear data transmission among secondary users (SUs) by reusing licensed spectrum without harming the benefits of authorized users (also known as primary users, PUs). Orthogonal frequency division multiplexing (OFDM) supports a flexible spectrum management by dividing the available spectrum into fine-granularity subcarriers and hence is recognized as a promising technology for spectrum reusing [5]. As a result, it is meaningful to combine CR and OFDM together and investigate new transmission paradigm in OFDM-based CR systems.

Meanwhile, energy efficiency (EE) is also a key metric for 5G, in which energy consumption needs to be reduced on the order of several magnitudes [6]. Note that extra power consumption incurred by spectrum sensing makes the power saving issue more critical in CR systems [7, 8]. Until now, large amounts of researches have been conducted to study energy-efficient transmission in OFDM-based CR systems. For example, in our early work [9], the EE metric measured by the achieved transmission bits per Joule is adopted, and the optimal power allocation for EE maximization is derived using *fractional programming*. Subsequently, the model is improved with the minimum rate guarantee and subcarrier assignment taken into account in [10, 11], respectively. Then, the authors in [12] further consider channel uncertainty and study the EE maximization problem with a probabilistic interference control policy.

However, all these researches mentioned above focus on unicast transmission. Along with the proliferation of smart phones, mobile multimedia services, especially mobile video services, have been in the explosive growth [13]. CR can effectively alleviate the more and more serious spectrum scarcity issue and is one of the key candidate technologies in 5G. Hence, it is almost an inevitable trend to deliver the increasing popular video services in the future communication system without licensed spectrum. Even for networks which have already been allocated with some spectrum bands, integrating CR function into the networks, for example, Licensed-Assisted Access (LAA) [14], can provide more competent video transmission, improving the user experience greatly. Moreover, as secondary networks can only access the authorized spectrum opportunistically, its transmission capacity is limited by the prioritized access mode. Hence, it is more challenging to transmit "*bandwidth-hungry*" video services with QoS guarantee in CR networks. The achieved results can provide a good guidance for how to bear other types of services in CR networks.

Video multicast has become an indispensable part for wireless networks, and hence it is of great significance to study how to scalably multicast video in CR systems. Several kinds of multicast schemes have been proposed for video transmission in the literature, including conventional multicast (CM) [13, 15], multiple description coding multicast (MDCM) [16, 17], and layered video multicast (LVM) [18, 19]. In CM [15], all subscribers in a multicast group receive the intended content with the identical quality, and the transmission rate is limited by the least channel gain of all subscribers. To cope with this issue, MDCM and LVM introduce source coding to support distinguished video transmission for different subscribers. In MDCM [16, 17], the video data is encoded into multiple descriptions and transmitted at different rates. For subscribers of various channel conditions, different sets of descriptions are received to jointly recover video with different resolutions. Despite being attractive in terms of system throughput, MDCM cannot guarantee the successful reception of key information and hence applies poorly in practice. By comparison, in LVM [18, 19], the video data is encoded into a base layer (BL) and several enhancement layers (ELs). The BL is intended to all subscribers at a low rate and hence can guarantee a basic recovered video quality, while the ELs are transmitted at incremental rates and opportunistically received by subscribers with promising channel conditions to persistently improve the video quality.

To the best our knowledge, existing researches on video multicast in OFDM-based CR systems mainly focus on CM [13, 15] or MDCM [16, 17], and what is more, only SE maximization model is studied. In this paper, joint intersession/interlayer subcarrier assignment and power allocation problem for energy-efficient LVM are studied in OFDM-based CR systems. For existing energy-efficient transmission models [9–12], *full-buffer* traffic model is assumed; that is, there is always infinite data waiting for transmission, and EE maximization is studied with no consideration of service characteristic. For LVM, the final recovered video quality is not linear with the receiving rate. Therefore, a utility function is introduced in our model to depict the relationship between the user experience, that is, recovered video quality, and its receiving rate, and a more accurate performance metric, *energy utility* (EU), is designed to measure the sum user experience achieved per Joule.

In detail, the main contributions of this paper can be summarized as follows.

(1) *EU-Based Optimization Model*. A novel optimization model is established for energy-efficient LVM in OFDM-based CR systems which aims at maximizing the system EU to balance the total recovered video quality and power consumption while guaranteeing multiple interference constraints for PUs.

(2) *Spectrum Assignment Method for LVM*. Both BL and EL subcarrier assignment algorithms are proposed to execute the intersession/interlayer subcarrier assignment in LVM. The BL subcarrier assignment aims at guaranteeing the basic video qualities for all multicast sessions with as fewer subcarriers as possible, while the EL subcarrier assignment tries to optimize the system EU by assigning subcarriers to the proper subscribers.

(3) *Optimal Power Allocation Method for EU Maximization*. For the multiconstrained EU-maximization problem, an optimal power allocation algorithm is presented by jointly utilizing fractional programming and subgradient method, which can be considered as the framework of optimizing energy-aware video multicast in OFDM-based CR systems.

The rest of the paper is organized as follows. In Section 2, we build the EU-based optimization model for LVM over OFDM-based CR systems. The subcarrier assignment for BL as well as EL and the EU-based power allocation are proposed and discussed by Section 3. Finally, simulation results are shown in Section 4, and conclusions are drawn in Section 5.

2. System Model and Problem Formulation

In this section, the spectrum division manner and the mutual-interference model are depicted firstly, and then the energy-efficient LVM transmission model is formulated with the objective of EU maximization.

2.1. OFDM-Based CR System. The considered CR system is composed of a primary network and a CR network, which are both deployed in a cellular fashion. The primary network consists of a primary base station (BS) and L PUs, while the CR network is made up of a secondary BS and K SUs. The whole licensed spectrum spans B Hz, and each PU occupies a disjoint fraction of the spectrum, denoted as B_l. For the finer-grained spectrum utilization, the OFDM technology is adopted to divide the whole sensed spectrum B into N subcarriers, with each subcarrier spanning $B_0 = B/N$ Hz [5, 9]. Figure 1 illustrates the details of CR system and spectrum distribution.

Since the sensed spectrum by CR network is licensed to the primary network, the privilege of PUs to use the spectrum must be guaranteed, which typically necessitates

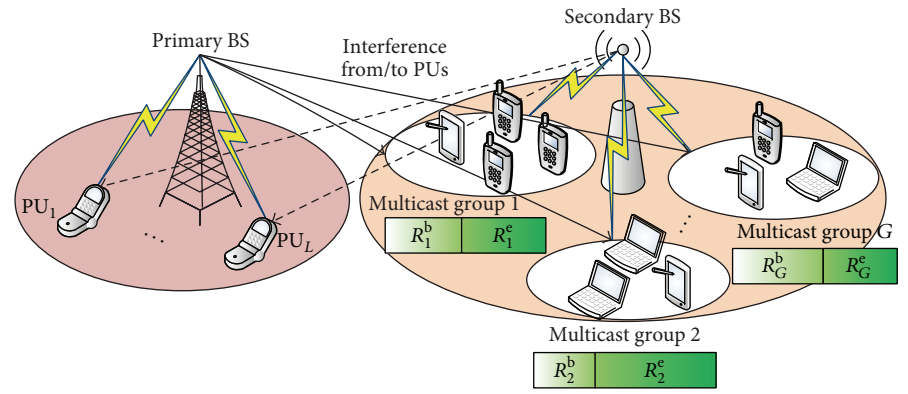

(a) CR system: a primary network and a CR network coexist

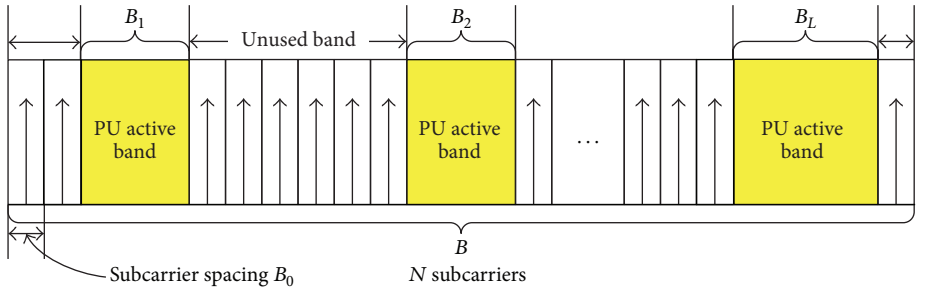

(b) Spectrum division by OFDM and spectrum occupation of PUs

Figure 1: System scenario and spectrum distribution.

the interference control. Therefore, a common interference evaluation model is introduced from [20].

In [19], the power spectrum density (PSD) of subcarrier n is written as

$$\varphi_n(f) = p_n T_s \left(\frac{\sin \pi f T_s}{\pi f T_s}\right)^2, \tag{1}$$

where p_n is the transmitted power of signal on subcarrier n and T_s is the duration of OFDM symbol. Then, the interference introduced by the signal on subcarrier n into PU l can be expressed as

$$\tilde{I}_{l,n}^{\mathrm{SP}} = G_l^{\mathrm{SP}} \int_{d_{l,n}-B_l/2}^{d_{l,n}+B_l/2} \varphi_n(f)\, df = I_{l,n} p_n, \tag{2}$$

where $d_{l,n}$ denotes the spectral distance between subcarrier n and the center frequency of PU l, G_l^{SP} denotes the channel gain from the secondary BS to PU l, and $I_{l,n}$ represents the interference caused by the normalized power on subcarrier n to PU l.

Meanwhile, the interference caused by the primary BS to SU k on subcarrier n is calculated as [20]

$$\tilde{I}_{k,n}^{\mathrm{PS}} = \sum_{l=1}^{L} G_{k,n}^{\mathrm{PS}} \int_{d_{l,n}-\Delta f/2}^{d_{l,n}+\Delta f/2} E\left[I_l(\omega)\right] d\omega, \tag{3}$$

where $G_{k,n}^{\mathrm{PS}}$ denotes the channel gain from primary BS to SU k on subcarrier n, and $E[\cdot]$ is the expectation operator. $E[I_l(\omega)]$ is the signal PSD of PU l after N-Fast-Fourier-transform (FFT) processing, and it is represented as

$$E\left[I_l(\omega)\right] = \frac{1}{2\pi N} \int_{-\pi}^{\pi} \Phi_l\left(e^{j\phi}\right) \left(\frac{\sin\left(\omega-\phi\right) N/2}{\sin\left(\omega-\phi\right)/2}\right)^2 d\phi, \tag{4}$$

where $\Phi_l(e^{j\phi})$ is the PSD of the transmitted signal by the primary BS to PU l, which is generally modeled as an elliptically filtered white noise process [20].

2.2. LVM Transmission Model. As shown in Figure 1(a), all K users are partitioned into G multicast groups according to the video contents they are interested in. The set and number of SUs in group g are denoted as $\mathcal{K}_g$ and $|\mathcal{K}_g|$, respectively. Let $H_{k|g,n}^{\mathrm{SS}}$ denote the channel gain between the secondary BS and SU k in group g, and the corresponding channel gain to interference-plus-noise ratio (CINR) can be expressed as

$$\gamma_{k|g,n} = \frac{H_{k|g,n}^{\mathrm{SS}}}{\sigma_n^2 + \tilde{I}_{k|g,n}^{\mathrm{PS}}}, \tag{5}$$

where σ_n^2 is the noise power on subcarrier n and $\tilde{I}_{k|g,n}^{\mathrm{PS}}$ is calculated according to (3) with an index mapping from $k \mid g$

to k. Based on the Shannon formula, the achievable data rate of SU k in group g on subcarrier n is calculated by

$$r_{k|g,n} = B_0 \log_2 \left(1 + p_n \gamma_{k|g,n}\right). \quad (6)$$

For CM, the lowest rate of SUs in a group is conservatively adopted to ensure the correct data reception of all SUs [15]. Thus, the data transmission rate of group g on subcarrier n is expressed as

$$r^{\mathrm{c}}_{g,n} = \min_{k \in \mathcal{K}_g} r_{k|g,n} = B_0 \log_2 \left(1 + p_n \min_{k \in \mathcal{K}_g} \gamma_{k|g,n}\right). \quad (7)$$

In wireless transmission, the heterogeneity of the receiving channels for different SUs will seriously limit the performance for CM. In order to overcome the shortcomings, LVM [18, 19] is introduced and modeled in this paper. In LVM, video data are transmitted resiliently on different subcarriers to adapt to the diverse channel conditions. This is accomplished by coding the source data into a BL and several ELs, and as long as the BL is received, SU can decode the video stream with the basic quality. If more ELs are received, the decoded video quality is increasingly improved [21]. The essential difference between CM and LVM lies in that the former requires that all SUs in a group receive the video with the identical quality, whilst the latter allows the differential reception, depending on the individual channel quality. Therefore, LVM provides a new degree of freedom, that is, the transmission rates on subcarriers, to exploit different channel conditions.

Specifically, it is assumed that each video g, which is received by group g, is encoded into one BL with rate R^{b}_g and one EL with rate R^{e}_g (see Figure 1(a)). $R^{\max}_g = R^{\mathrm{b}}_g + R^{\mathrm{e}}_g$ denotes the maximal rate for video g. As in [19], we also assume that the fine grained scalability (FGS) coding technique is adopted, so that the EL can be truncated at any bit location with all the remaining bits still being useful at the decoder [22].

In LVM, the BL data is of great importance to reconstruct the source video, and it is imperative that the BL can be received by all the SUs in a group. Hence, if subcarrier n is used by group g for the BL transmission, the transmission rate is equal to that of CM; that is,

$$r^{\mathrm{b}}_{g,n} = r^{\mathrm{c}}_{g,n}. \quad (8)$$

If subcarrier n is used by group g for the EL transmission at a rate of $r^{\mathrm{e}}_{g,n}$, the receiving rate of SU $k, k \in \mathcal{K}_g$ on subcarrier n is written as

$$\sigma\left(r_{k|g,n} \geq r^{\mathrm{e}}_{g,n}\right) r^{\mathrm{e}}_{g,n}, \quad (9)$$

where $\sigma(T)$ is 1 if T is true, otherwise 0. Define two indicators $\rho_{g,n}$ and s_n to perform the intersession and interlayer subcarrier assignment as follows. $\rho_{g,n} \in \{1, 0\}$ denotes whether subcarrier n is assigned to group g or not, and s_n denotes whether subcarrier n is used for the BL transmission ($s_n = 1$) or the EL transmission ($s_n = 0$). The achieved rate of SU $k, k \in \mathcal{K}_g$ is calculated as

$$R_k = \sum_{n=1}^{N} \rho_{g,n} \left[\left(1 - s_n\right) \sigma\left(r_{k|g,n} \geq r^{\mathrm{e}}_{g,n}\right) r^{\mathrm{e}}_{g,n} + s_n r^{\mathrm{b}}_{g,n}\right]. \quad (10)$$

2.3. EU-Based Problem Formulation. In LVM, the achieved rate cannot reflect the quality directly, and some metrics, such as peak signal to noise ratio (PSNR) and mean square error (MSE), may be more accurate to evaluate the received video quality. For generalizing the expression, the utility function $U_k(R_k)$ is defined to denote the change relationship of reconstructed video quality with the achieved rate. Moreover, $U_k(R_k)$ is assumed to be nondecreasing and concave according to the measured or theoretical results [18, 19]. Then, the total weighted-utility is summed as

$$U_{\mathrm{total}} = \sum_{k=1}^{K} w_k U_k\left(R_k\right), \quad (11)$$

where w_k ($w_k > 0$) is the weight of SU k and can be used to reflect the relative priorities among SUs.

Apart from the video quality, the energy cost of video transmission over OFDM-based CR systems should be also considered. The total energy consumption in a timeslot includes three parts: the sense energy P_{s}, that is, the energy consumed to sense the available spectrum, the transmission energy P_{t}, that is, the energy consumed to transmit data on the sensed spectrum, and the circuit energy P_{c}. Note that the concepts of "*energy*" and "*power*" are not strictly distinguished in this paper, since only the constant duration is multiplied or not. The total energy consumption is accumulated as

$$E_{\mathrm{total}} = P_{\mathrm{t}} + P_{\mathrm{s}} + P_{\mathrm{c}} = \sum_{n=1}^{N} p_n + \xi \sum_{n=1}^{N} p_n + P_{\mathrm{c}}, \quad (12)$$

where ξ denotes the ratio of the sense energy P_{s} to the transmission energy P_{t} [15]. The formula accounts for the required energy consumption for downlink (DL) video multicast in OFDM-based CRNs. In practice, the total system power consumption includes the power consumption at both BS and end device sides. The power consumption of end devices during DL transmission mainly results from multiple active circuit modules, such as the channel estimation and feedback module and the baseband signal processing module. However, the aggregate value is relatively small compared with the power consumption of BS, whose radio frequency (RF) transmit power is often very large due to the large-scale pathloss fading. As a result, the power consumption of end devices is not considered in formula (12), in which the total system energy consumption is approximated as the power consumption at the secondary BS [7, 9–12].

In the existing work, EE is maximized to optimize the achieved rate by the unit energy consumption [9–12]. For the video transmission, it makes more sense to shift EE to

EU. Therefore, the EU-based video transmission problem is formulated as

$$\begin{aligned}
\mathcal{OP}_0: \quad & \max_{\rho_{g,n},p_n,s_n,r^{\mathrm{e}}_{g,n},r^{\mathrm{b}}_{g,n}} \eta_{\mathrm{EU}} = \frac{U_{\mathrm{total}}}{E_{\mathrm{total}}} \\
& C_1\colon \sum_{n=1}^{N} p_n \le P_{\mathrm{total}} \\
& C_2\colon \sum_{n=1}^{N} I_{l,n} p_n \le I^l_{\mathrm{th}}, \quad 1 \le l \le L \\
& C_3\colon p_n \ge 0, \quad 1 \le n \le N \\
& C_4\colon \sum_{n=1}^{N} \rho_{g,n} s_n r^{\mathrm{b}}_{g,n} \ge R^{\mathrm{b}}_g, \quad 1 \le g \le G \\
& C_5\colon \sum_{g=1}^{G} \rho_{g,n} \le 1, \quad 1 \le n \le N \\
& C_6\colon \rho_{g,n} \in \{0,1\}, \quad 1 \le n \le N,\ 1 \le g \le G \\
& C_7\colon s_n \in \{0,1\}, \quad 1 \le n \le N,
\end{aligned} \tag{13}$$

where P_{total} is the total transmitted power by the secondary BS and I^l_{th} is the interference threshold for PU l. In $\mathcal{OP}_0$, C_2 denotes the total interference constraint from each PU, C_4 requires that the BL data can be received by all the SUs in each group to guarantee the basic quality of reconstructed video, and C_5 and C_6 restrict that one subcarrier is exclusively used by only one group, since different groups may be interested in distinct video contents from the secondary BS. It is assumed that the secondary BS has the perfect knowledge of multicast grouping, the bandwidth of B, channel gains, and interference coefficients.

3. Optimized Video Multicast Transmission

In order to achieve the optimal performance, spectrum assignment $\rho_{g,n}$, s_n, power allocation p_n, and the data transmission rate selection $r^{\mathrm{e}}_{g,n}$, $r^{\mathrm{b}}_{g,n}$ should be jointly determined. Nevertheless, the tight coupling among these variables will incur a prohibitively high computation complexity. Therefore, allowing for the features of LVM and CRN, we decompose $\mathcal{OP}_0$ into three steps, that is, BL subcarrier assignment, EL subcarrier assignment, and power allocation. Additionally, how to deal with the spectrum scarcity is also discussed.

3.1. BL Subcarrier Assignment. For unifying the expression, let $I_{0,n} = 1$, $1 \le n \le N$, $I^0_{\mathrm{th}} = P_{\mathrm{total}}$. In the traditional OFDM systems, where no primary network exists, equal power P_{total}/N is generally assumed for subcarrier assignment [23]. In OFDM-based CRNs, the interference to PUs has to be considered, and the interference coefficient $I_{l,n}$ varies from one subcarrier to another. The coarse assumption of equal power deviates from the actual situations and may degrade the performance. Instead, the ladder-profile power is assumed in this paper:

$$p_n = \min\left(\frac{I^0_{\mathrm{th}}}{NI_{0,n}}, \frac{I^1_{\mathrm{th}}}{NI_{1,n}}, \ldots, \frac{I^L_{\mathrm{th}}}{NI_{L,n}}\right). \tag{14}$$

This idea is borrowed from [24], which supposes that each subcarrier produces the identical amount of interference to PUs. Obviously, the power p_n in (14) rests with the interference coefficients and may differ among subcarrier individuals. It can be verified that all the power and interference constraints C_1 and C_2 are satisfied by (14); that is, $\sum_{n=1}^{N} I_{l,n} p_n \le \sum_{n=1}^{N} I_{l,n}(I^l_{\mathrm{th}}/NI_{l,n}) \le I^l_{\mathrm{th}}$ for $0 \le l \le L$. Furthermore, a factor $\beta \le 1$ is calculated to scale the power p_n as

$$\beta = \max_{0 \le l \le L} \frac{\sum_{n=1}^{N} I_{l,n} p_n}{I^l_{\mathrm{th}}}, \quad p_n = \frac{p_n}{\beta}, \tag{15}$$

such that at least one constraint in C_1, C_2 is active for maintaining the reasonable power level.

With (14) and (15), the achievable rate $r^{\mathrm{b}}_{g,n}$ of BL is readily computed according to (7) and (8). The details of BL subcarrier assignment are provided in Algorithm 1. The objective of Algorithm 1 is to meet the BL rate requirements with as small number of subcarriers as possible. At each iteration, the most unsatisfied group g with the largest gap from the BL rate requirement is selected, and then the best subcarrier n with the largest achievable rate is assigned to this group. Subsequently, the state of whether the rate requirement is fulfilled or not is inspected for group g, and if satisfied, it is immediately removed from the set of unsatisfied groups $\mathcal{G}$ to save more subcarriers for EL data transmission.

Either $\mathcal{A} = \varnothing$ or $\mathcal{G} = \varnothing$ will terminate Algorithm 1. However, only when $\mathcal{A} \ne \varnothing$, that is, there is a surplus of subcarriers, EL subcarrier assignment is needed, which progressively improves the quality of video.

3.2. EL Subcarrier Assignment. For EL subcarrier assignment, besides the task of assigning subcarriers to the appropriate groups, the data transmission rate $r^{\mathrm{e}}_{g,n}$ should also be determined jointly. In $\mathcal{OP}_0$, $r^{\mathrm{e}}_{g,n}$ is limited to be a nonnegative real number. It seems that the derivative method has to be adopted to obtain the optimal $r^{\mathrm{e}}_{g,n}$ as the value of $r^{\mathrm{e}}_{g,n}$ is continuous. However, by a close observation, $r^{\mathrm{e}}_{g,n}$ can only take finite $K + 1$ values. Specifically, the following theorem is presented to reduce the complexity of subcarrier assignment for EL.

Theorem 1. *With the nondecreasing utility functions, for any subcarrier n assigned to transmit the EL data, the optimal rate $r^{e}_{g,n}$ is equal to* 0 *or $r^{e}_{g,n} \in \mathcal{B}_n = \{r_{m|g,n} \mid 1 \le g \le G,\ m \in \mathcal{K}_g\}$; that is, $r^{e}_{g,n}$ must be zero or one of the K achievable rates in $\mathcal{B}_n$.*

Proof. See Appendix A. □

Theorem 1 indicates that if subcarrier n is assigned to group g, then only the $|\mathcal{K}_g|$ achievable rates may be the

Input:
(1) P_{total}, $\gamma_{m|g,n}$ for $m \in \mathscr{K}_g$, $1 \le g \le G$, p_n for $1 \le n \le N$, $I_{l,n}$ for $1 \le l \le L$, $1 \le n \le N$, I_{th}^l for $1 \le l \le L$, and R_g^{b} for $1 \le g \le G$;
Initialization:
(2) Initialize the set of BL-rate-unsatisfied groups $\mathscr{G} = \{1, 2, \ldots, G\}$, the set of unassigned subcarriers $\mathscr{A} = \{1, 2, \ldots, N\}$, the achieved rate $\widetilde{R}_g = 0$ for group g, the set of assigned subcarriers $\Omega_k = \varnothing$ for SU k, the assignment indicator $\rho_{g,n} = 0$, $1 \le n \le N$, $1 \le g \le G$;
Iteration:
(3) **while** $\mathscr{A} \neq \varnothing$ **and** $\mathscr{G} \neq \varnothing$ **do**
(4) Find group $g \in \mathscr{G}$ satisfying $\widetilde{R}_g - R_g^{\text{b}} \le \widetilde{R}_i - R_i^{\text{b}}$, $\forall i \in \mathscr{G}$;
(5) Select subcarrier n to maximize the achieved rate as $n = \arg\max_j r_{g,j}^{\text{b}}$, $j \in \mathscr{A}$;
(6) Assign subcarrier n to group g for BL data transmission as $\rho_{g,n} = 1$, $\mathscr{A} = \mathscr{A} - \{n\}$, $s_n = 1$, and update $\widetilde{R}_g$, Ω_k as $\widetilde{R}_g = \widetilde{R}_g + r_{g,n}^{\text{b}}$, $\Omega_k = \Omega_k \cup \{n\}$, $\forall k \in \mathscr{K}_g$;
(7) **if** $\widetilde{R}_g \ge R_g^{\text{b}}$ **then**
(8) Delete group g as $\mathscr{G} = \mathscr{G} - \{g\}$;
(9) **end if**
(10) **end while**
Output:
(11) $\mathscr{G}, \mathscr{A}, \widetilde{R}_g, \Omega_k, \rho_{g,n}, s_n$.

Algorithm 1: Algorithm for BL subcarrier assignment.

Input:
(1) $w_k, \xi, P_c, P_{\text{total}}, \gamma_{m|g,n}$ for $m \in \mathscr{K}_g$, $1 \le g \le G, n \in \mathscr{A}$, p_n for $n \in \mathscr{A}$, $I_{l,n}$ for $1 \le l \le L, n \in \mathscr{A}$ and I_{th}^l for $1 \le l \le L$;
Initialization:
(2) Initialize the set of unassigned subcarriers $\mathscr{A}$, the set of assigned subcarriers Ω_k for SU k, and the assignment indicator $\rho_{g,n}, n \notin \mathscr{A}, 1 \le g \le G$ according to the output of Algorithm 1. Set $\rho_{g,n} = 0$, $n \in \mathscr{A}$, $1 \le g \le G$, and the achieved rate $R_k = \widetilde{R}_g$ for SU k, $k \in \mathscr{K}_g$;
Iteration:
(3) **while** $\mathscr{A} \neq \varnothing$ **do**
(4) Select subcarrier $n, n \in \mathscr{A}$ in order, and find group g and BU m to maximize the achieved EU as $(g, m) = \arg\max_{\rho_{i,n}, r_{j|i,n}} \eta_{\text{EU}}$, $1 \le i \le G$, $j \in \mathscr{K}_g$;
(5) Assign subcarrier n to group g for EL data transmission as $\rho_{g,n} = 1$, $\mathscr{A} = \mathscr{A} - \{n\}$, $s_n = 0$, and update R_k, Ω_k as $R_k = R_k + \sigma(r_{k|g,n} \ge r_{m|g,n}) r_{m|g,n}$ for $k \in \mathscr{K}_g$, $\Omega_k = \Omega_k \cup \{n\}$ for $r_{k|g,n} \ge r_{m|g,n}$, $k \in \mathscr{K}_g$;
(6) **end while**
Output:
(7) $\Omega_k, \rho_{g,n}, s_n, r_{m|g,n}$.

Algorithm 2: Algorithm for EL subcarrier assignment.

optimal solution. In total, all $K = \sum_{g=1}^{G} |\mathscr{K}_g|$ achievable rates constitute the candidates for the optimal solution if subcarrier n is not assigned yet. This contracts the domain of $r_{g,n}^{\text{e}}$ from the nonnegative real number to $K + 1$ discrete values and thereby eases the determination process of $r_{g,n}^{\text{e}}$. Define SU m as the barrier user (BU) on subcarrier n if its achievable rate is selected for data transmission, that is, $r_{g,n}^{\text{e}} = r_{m|g,n}$, since its rate marks the watershed between the success and failure in data reception. According to Theorem 1, the rate of SU k in (10) is rewritten as

$$R_k = \sum_{n=1}^{N} \rho_{g,n} \left[(1 - s_n)\, \sigma\left(r_{k|g,n} \ge r_{m|g,n}\right) r_{m|g,n} + s_n r_{g,n}^{\text{b}} \right], \tag{16}$$

where BU m may be different among subcarriers and needs to be decided by Algorithm 2.

The objective of Algorithm 2 is to maximize the EU via subcarrier assignment for EL. At each iteration, subcarrier n is selected in order, and then, based on Theorem 1, the traversal of $K + 1$ values for $r_{g,n}^{\text{e}}$ is carried out in order to achieve the maximal EU η_{EU}. In Algorithm 2, for $1 \le i \le G$, $j \in \mathscr{K}_g$, to maximize η_{EU} is equivalent to maximizing the total utility as

$$\arg \max_{\rho_{i,n}, r_{j|i,n}} \eta_{\text{EU}} = \arg \max_{\rho_{i,n}, r_{j|i,n}} \sum_{k=1}^{K} w_k U_k\left(R_k\right), \tag{17}$$

since the power consumption values are equal for the denominator of η_{EU} when determining which group subcarrier n is assigned to and which SU is selected as the BU.

3.3. EU-Based Power Allocation. With the determined subcarrier assignment, the rate of SU $k, k \in \mathscr{K}_g$ in (16) can be further expressed as

$$\begin{aligned} R_k &= \sum_{n\in\Omega_k}\left[(1-s_n)\, r_{m|g,n} + s_n r^{\mathrm{b}}_{g,n}\right] = \sum_{n\in\Omega_k} r_n \\ &= \sum_{n\in\Omega_k} B_0 \log_2\left(1+p_n\gamma_n\right), \end{aligned} \tag{18}$$

where r_n and γ_n are the achievable rate and CINR, respectively, for the BU related to subcarrier n in group g. Note that if subcarrier n is used for EL, the BU is specified in Algorithm 2. Otherwise, for BL, the BU is the SU in group g with the worst channel condition on subcarrier n.

When determining subcarrier assignment, the ladder-profile power is simply assumed in (14) and (15) to evaluate the rate or utility in Algorithms 1 and 2. Thus, the power needs to be reallocated to maximize the EU for multicast video transmission, which is formulated as

$$\begin{aligned} \mathscr{OP}_1\colon\quad & \max_{p_n} \eta_{\mathrm{EU}}(\mathbf{p}) = \frac{U_{\mathrm{total}}(\mathbf{p})}{E_{\mathrm{total}}(\mathbf{p})} \\ & C_1\colon \sum_{n=1}^{N} p_n \le P_{\mathrm{total}} \\ & C_2\colon \sum_{n=1}^{N} I_{l,n} p_n \le I^l_{\mathrm{th}}, \quad 1\le l\le L \\ & C_3\colon\ p_n \ge 0, \quad 1\le n\le N \\ & C_4\colon \sum_{n\in\Theta^{\mathrm{b}}_g} r_n \ge R^{\mathrm{b}}_g, \quad 1\le g\le G, \end{aligned} \tag{19}$$

where Θ^{b}_g is the set of subcarriers assigned to group g for the BL transmission and $\mathbf{p}$ denotes the vector of p_n, $1 \le n \le N$. Even though the optimization variables associated with subcarrier assignment in $\mathscr{OP}_0$ have been settled, $\mathscr{OP}_1$ is still intractable due to the fractional objective function as well as a large number of constraints on the power and BL rate.

As in our previous work [9], *fractional programming* [25] is employed to deal with the objective function issue. With the positive parameter α, a new function $g(\mathbf{p},\alpha)$ is defined as

$$g(\mathbf{p},\alpha) = E_{\mathrm{total}}(\mathbf{p}) - \alpha U_{\mathrm{total}}(\mathbf{p}). \tag{20}$$

Then, another problem is formulated as

$$\begin{aligned} \mathscr{OP}_2\colon\quad & \min_{p_n} g(\mathbf{p},\alpha) \\ & C_1, C_2, C_3, C_4. \end{aligned} \tag{21}$$

Let S denote the feasible region of $\mathscr{OP}_1$ and $\mathscr{OP}_2$, and define the optimal value and solution of $\mathscr{OP}_2$ as

$$\begin{aligned} F(\alpha) &= \min_{\mathbf{p}} \{g(\mathbf{p},\alpha) \mid \mathbf{p}\in S\}, \\ \mathbf{f}(\alpha) &= \arg\min_{\mathbf{p}} \{g(\mathbf{p},\alpha) \mid \mathbf{p}\in S\}. \end{aligned} \tag{22}$$

The following lemma can relate $\mathscr{OP}_1$ and $\mathscr{OP}_2$, and the detailed proof of Lemma 2 can be found in [25].

Lemma 2. *$\mathbf{p}^*$ and $1/\alpha^*$ correspond to the optimal solution and value of problem $\mathscr{OP}_1$ in (19); that is, $1/\alpha^* = U_{total}(\mathbf{p}^*)/E_{total}(\mathbf{p}^*) = \max_{\mathbf{p}}\{\eta_{EU}(\mathbf{p}) \mid \mathbf{p}\in S\}$, if and only if*

$$\begin{aligned} F(\alpha^*) &= 0, \\ \mathbf{f}(\alpha^*) &= \mathbf{p}^*. \end{aligned} \tag{23}$$

Lemma 2 indicates that the optimal solution to $\mathscr{OP}_2$ is also the optimal solution to $\mathscr{OP}_1$, provided that (23) is satisfied. Hence, solving $\mathscr{OP}_1$ can be realized by finding the optimal power allocation of $\mathscr{OP}_2$ for a given α, and then update α until (23) is established. The problem at hand is how to achieve the optimal power allocation for $\mathscr{OP}_2$ with a given α. To this end, the following theorem is presented.

Theorem 3. *If the utility function is nondecreasing and concave for each SU, problem $\mathscr{OP}_2$ with a fixed α belongs to convex optimization ones.*

Proof. See Appendix B. □

The convexity of $\mathscr{OP}_2$ with a fixed α enables the solution in the dual domain without the dual gap [26]. Namely, the optimal solution to the dual problem is exactly the optimal solution to the primal problem $\mathscr{OP}_2$. The Lagrangian of $\mathscr{OP}_2$ is defined as

$$\begin{aligned} L = {} & E_{\mathrm{total}}(\mathbf{p}) - \alpha U_{\mathrm{total}}(\mathbf{p}) + \sum_{l=0}^{L}\lambda_l\left(\sum_{n=1}^{N} I_{l,n}p_n - I^l_{\mathrm{th}}\right) \\ & + \sum_{g=1}^{G}\upsilon_g\left(R^{\mathrm{b}}_g - \sum_{n\in\Theta^{\mathrm{b}}_g} r_n\right), \end{aligned} \tag{24}$$

where $\boldsymbol{\lambda} = [\lambda_0, \lambda_1, \ldots, \lambda_L] \succeq \mathbf{0}$ and $\boldsymbol{\upsilon} = [\upsilon_1, \ldots, \upsilon_G] \succeq \mathbf{0}$ are vectors of dual variables. Therefore, its dual function is defined as

$$h(\boldsymbol{\lambda}, \boldsymbol{\upsilon}, \alpha) = \min_{p_n} L. \tag{25}$$

According to the Karush-Kuhn-Tucker (KKT) conditions [26], the optimal power allocation should satisfy

$$\begin{aligned} \frac{\partial L}{\partial p_n} = {} & \left[-\alpha\sum_{k\in\Phi_n} w_k \frac{dU_k(R_k)}{dR_k} - s_n\upsilon_g\right]\frac{B_0}{\ln 2}\frac{\gamma_n}{1+p_n\gamma_n} \\ & + \sum_{l=0}^{L}\lambda_l I_{l,n} + \xi + 1 = 0, \end{aligned} \tag{26}$$

where Φ_n denotes the set of SUs who can receive data from subcarrier n. By some manipulations, the optimal p_n is derived as

$$\begin{aligned} p_n = {} & \left[\frac{B_0}{\ln 2}\frac{\alpha\sum_{k\in\Phi_n} w_k\left(dU_k(R_k)/dR_k\right) + s_n\upsilon_g}{\sum_{l=0}^{L}\lambda_l I_{l,n} + \xi + 1}\right. \\ & \left. - \frac{1}{\gamma_n}\right]^+, \end{aligned} \tag{27}$$

Input:
(1) $w_k, \xi, P_c, P_{\text{total}}, \gamma_{m|g,n}$ for $m \in \mathcal{K}_g$, $1 \le g \le G$, $1 \le n \le N$, $I_{l,n}$ for $1 \le l \le L$, $1 \le n \le N$, I_{th}^l for $1 \le l \le L$, Ω_k for $1 \le k \le K$, Φ_n, s_n for $1 \le n \le N$ and $\Theta_g^{\text{b}}, R_g^{\text{b}}$ for $1 \le g \le G$;
Initialization:
(2) Initialize α, and the tolerable error ϵ. Set $F(\alpha) = \infty$;
Iteration:
(3) **while** $|F(\alpha)| > \epsilon$ **do**
(4) Initialize the tolerable error $\widetilde{\epsilon}$, the dual variables λ_l, $0 \le l \le L$, υ_g, $1 \le g \le G$, and $e = \infty$;
(5) **while** $e > \widetilde{\epsilon}$ **do**
(6) Calculate p_n according to (26) or (27);
(7) Update λ_l, υ_g according to (29);
(8) Compute e as $e = \|\Delta\boldsymbol{\lambda}/\boldsymbol{\lambda}(t)\| + \|\Delta\boldsymbol{\upsilon}/\boldsymbol{\upsilon}(t)\|$ with $\Delta\boldsymbol{\lambda} = \boldsymbol{\lambda}(t+1) - \boldsymbol{\lambda}(t)$, $\Delta\boldsymbol{\upsilon} = \boldsymbol{\upsilon}(t+1) - \boldsymbol{\upsilon}(t)$;
(9) **end while**
(10) Compute $F(\alpha)$, and update $\alpha = E_{\text{total}}(\mathbf{p})/U_{\text{total}}(\mathbf{p})$;
(11) **end while**
Output:
(12) p_n and the final EU $\eta_{\text{EU}} = 1/\alpha$.

Algorithm 3: EU-based power allocation.

where $[x]^+$ denotes $\max\{0, x\}$. In general, the analytical expression of p_n is unavailable, except that $U_k(R_k)$ is linear with R_k for any SU k. In such cases, $dU_k(R_k)/dR_k$ is independent of p_n. Otherwise, n nonlinear equations with n unknowns in (26) have to be solved numerically to find the optimal p_n.

Once the optimal p_n is achieved, the dual function $h(\boldsymbol{\lambda}, \boldsymbol{\upsilon}, \alpha)$ in (25) can be computed for the fixed tuple $(\boldsymbol{\lambda}, \boldsymbol{\upsilon})$. Now, the dual problem needs to be solved as

$$\max_{\boldsymbol{\lambda}\ge\mathbf{0},\boldsymbol{\upsilon}\ge\mathbf{0}} h(\boldsymbol{\lambda}, \boldsymbol{\upsilon}, \alpha). \tag{28}$$

The optimal solution to (28) can be steadily obtained in a subgradient method [27], which iteratively updates the dual variables $(\boldsymbol{\lambda}, \boldsymbol{\upsilon})$ in the subgradient direction until they converge. Specifically, the updates for (28) can be performed as

$$\lambda_l(t+1) = \left[\lambda_l(t) - \varepsilon_t\left(I_{\text{th}}^l - \sum_{n=1}^{N} I_{l,n}p_n\right)\right]^+, \quad 0 \le l \le L,$$
$$\upsilon_g(t+1) = \left[\upsilon_g(t) - \omega_t\left(\sum_{n\in\Theta_g^{\text{b}}} r_n - R_g^{\text{b}}\right)\right]^+, \quad 1 \le g \le G, \tag{29}$$

where $\varepsilon_t, \omega_t > 0$ form two sequences of step sizes. In general, the step size ε_t, ω_t can be selected as κ/t or $\kappa/\sqrt{t}$ based on the diminishing rules [27], where $\kappa > 0$ is a constant, and t is the number of iterations. The subgradient method can guarantee that $(\boldsymbol{\lambda}, \boldsymbol{\upsilon})$ converges to the optimal point as long as ε_t and ω_t are sufficiently small [27]. Due to the convexity depicted by Theorem 3, the optimal solution to $\mathcal{OP}_2$ can be achieved according to (26) or (27) once the dual optimal solution $(\boldsymbol{\lambda}^*, \boldsymbol{\upsilon}^*)$ is reached.

With the optimal power allocation $\mathbf{p}$ for the given α, update $\alpha = E_{\text{total}}(\mathbf{p})/U_{\text{total}}(\mathbf{p})$ and solve problem $\mathcal{OP}_2$ again. The process is repeated until the condition of Lemma 2 is satisfied. The iteration convergence of α update is proved in [24]. The details of power allocation are provided in Algorithm 3, where $\|\mathbf{x}\|$ denotes the 2-norm of vector $\mathbf{x}$.

The objective of Algorithm 3 is to maximize the EU by allocating power among subcarriers, whilst guaranteeing the BL rate requirements. In the inner loop, power allocation $\mathbf{p}$ and dual variables $(\boldsymbol{\lambda}, \boldsymbol{\upsilon})$ are alternately updated to attain the optimal solution for a fixed α. In the outer loop, α is repeatedly updated until it converges. It can be asserted that Algorithm 3 can reap the optimal power for $\mathcal{OP}_1$, owing to the factor that both the inner-loop and outer-loop iterations can converge to the respective optimal solutions.

In a practical system, the video is encoded into data layers at first, and then the BL data is mapped onto subcarriers by Algorithm 1. Sequentially, the EL data is arranged on the unused subcarriers by Algorithm 2, and the power, corresponding to the transmission rate, for each subcarrier is ultimately settled by Algorithm 3. Through all three algorithms, the EU is consecutively optimized to deliver the video to diverse receivers with the detected spectrum and limited energy.

3.4. Spectrum Scarcity Discussion. Typically, the video service is "*bandwidth-hungry,*" and wireless network states, including channel quality, service requests, and the numbers of SUs and PUs, remain ever-changing. Sometimes the sensed spectrum is not enough for supporting the BL rates of all the groups. For example, the available bandwidth is overly narrow due to the full occupation of the primary network, or the interference threshold is excessively tight because the CR network is geographically close to the primary network. For such cases, problem $\mathcal{OP}_0$ has no feasible solutions, which is usually reflected by the phenomenon that Algorithm 1 stops with $\mathcal{A} = \varnothing$.

In order to address the issue, the *aggressive* solution is to drop some SUs according to the service emergency or the requested rate of BL data, and in the next timeslot, more transmission opportunities are offered to these sacrificed SUs. The *conservative* solution is to relax the BL rate constraint C_4 in $\mathcal{OP}_0$ and adaptively determine the transmission rates of each SU by its contribution to the EU η_{EU}; that is, the SU who can increase the total utility most by the unit energy consumption will achieve the transmission opportunity. This solution can restrain parts of SUs from data transmission in an "*EU-competitive*" fashion.

4. Simulation Results

In this section, channel fading gains from the secondary BS to SUs and PUs are modeled as consisting of six independent Rayleigh multipaths with an average channel power gain of 0 dB. The sensed spectrum is divided into $N = 64$ subcarriers with the subcarrier spacing $B_0 = 15$ KHz in frequency band. $L = 4$ PUs are assumed to be active in the primary network, and each PU occupies a fraction of spectrum with an equal bandwidth of $2B_0$. The locations of PU bands are assumed to evenly span the whole frequency band.

The noise power plus the interference power is identically set as σ_0^2 for each subcarrier, and the total transmission power is $P_{\text{total}} = 1$ W. The average signal to interference-plus-noise ratio (SINR), which is defined as $P_{\text{total}}/(N\sigma_0^2)$, ranges from 8 dB to 28 dB. The interference threshold of each PU $I_{\text{th}}^l = 0.5$ mW for $1 \le l \le L$. The weight $w_k = 1$, $1 \le k \le K$, is designated to maximize the system sum-utility. The circuit energy consumption $P_{\text{c}} = 0.1$ W, and the ratio of the sense energy to the transmission energy is set as $\xi = 0.1$.

In the CR network, two video sequences, that is, *Foreman* and *Harbour* in [18], are dedicated to $G = 2$ groups. The piecewise linear utility function [18] is selected to evaluate the PSNR performance as

$$U_k(r) = \begin{cases} U_g^0 + \chi_g\left(r - R_g^{\text{b}}\right) & r \le R_g^{\text{b}} \\ U_g^0 + \tau_g\left(r - R_g^{\text{b}}\right) & R_g^{\text{b}} < r \le R_g^{\max} \\ U_g^0 + \tau_g\left(R_g^{\max} - R_g^{\text{b}}\right) & r > R_g^{\max}, \end{cases} \tag{30}$$

where U_g^0, $k \in \mathcal{K}_g$, denotes the PSNR when only the BL data is received and χ_g and τ_g are the slopes of the two pieces. The parameters U_g^0, R_g^{b}, $R_g^{\max}$, χ_g, and τ_g are set according to the video sequences *Foreman* and *Harbour* in [18]. With the specific utility function (30), the optimal p_n in (27) can be rewritten as

$$p_n = \left[\frac{B_0}{\ln 2}\frac{\alpha\left(\sum_{k\in\Phi_n^{\text{L}}} w_k\chi_g + \sum_{k\in\Phi_n^{\text{M}}} w_k\tau_g\right) + s_n\upsilon_g}{\sum_{l=0}^{L}\lambda_l I_{l,n} + \xi + 1} - \frac{1}{\gamma_n}\right]^+, \tag{31}$$

where Φ_n^{L} and Φ_n^{M} are the subsets of Φ_n and denote the sets of SUs in Φ_n, whose total rate R_k, respectively, satisfies $R_k \le R_g^{\text{b}}$ and $R_g^{\text{b}} < R_k \le R_g^{\max}$. For comparison, another utility function $U_k(r) = r$ is also simulated to maximize the weighted-rate. All simulation results are averaged over 1000 channel realizations.

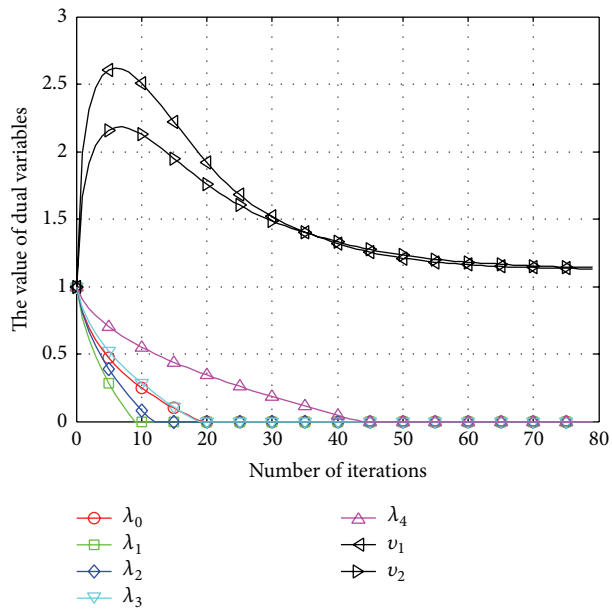

Figure 2: The convergence process of dual variables in the energy-utility-based power allocation algorithm.

Table 1: Average number of iterations for auxiliary variable α.

Optimization objective function	Weighted-PSNR	Weighted-rate
Average number of iterations	2.1	3.6

Figure 2 shows the convergence process of dual variables λ_l, $l = 0, 1, 2, 3, 4$, and υ_g, $g = 1, 2$, in the EU-based power allocation algorithm, where the number of SUs is 4 in each group, and the average SINR is equal to 12 dB. It can be observed that the dual variables rapidly converge to the stable points within 10~80 iterations. Table 1 lists the average iteration numbers of auxiliary variable α. No matter which objective function is optimized, weighted-PSNR or weighted-rate, approximately 2~4 iterations are sufficient to achieve the converged α, which indicates that the high convergence rate of α is little impacted by the objective function. Combining Figure 2 with Table 1, it is concluded that the EU-based power allocation algorithm possesses the favourable iteration complexity.

In Figure 3, the EEs of the CM [14] and LVM are demonstrated with the increase of the SU number in each group. That is, the utility function is chosen as $U_k(r) = r$. As the number of SUs increases, both multicast methods are capable of achieving the higher EE, due to the fact that more SUs can benefit from a single transmission. In the meantime, the EE gap between them continuously enlarges, because the LVM enables the differential data reception and breaks through the worst channel restraint in CM. For example, with

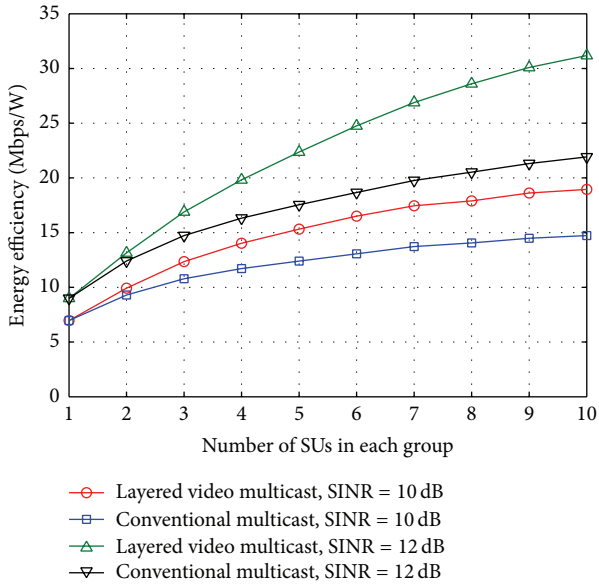

FIGURE 3: The energy efficiency comparison between the conventional multicast and layered video multicast.

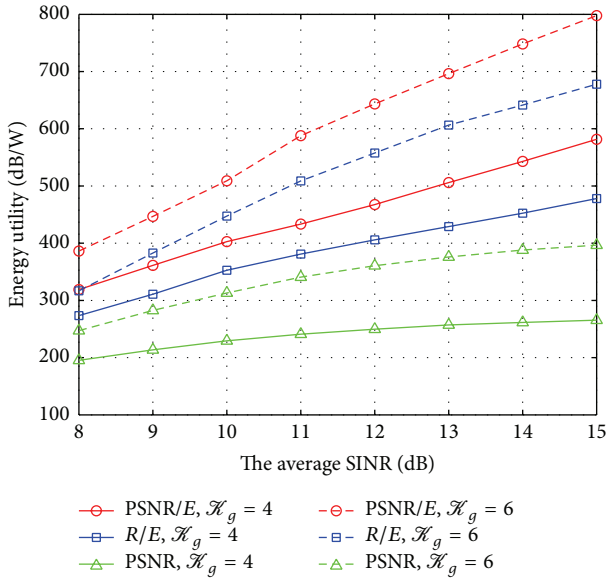

FIGURE 4: The energy utility comparison among different optimization objective functions.

SINR = 12 dB, when the number of SUs is 10 in each group, the EE gain is nearly up to 40%.

In Figure 4, we compare three optimization objective functions, that is, the EU (the weighted-PSNR divided by the total energy consumption), the EE (the weighted-rate divided by the total energy consumption) [9–12], and the weighted-PSNR [18, 19], for the video transmission in terms of the achieved PSNR by the unit energy consumption. From Figure 4, it can be seen that because of integrating the energy cost into consideration the EE optimization achieves a significant performance gain over the weighted-PSNR optimization. Moreover, the EU optimization is considerably superior

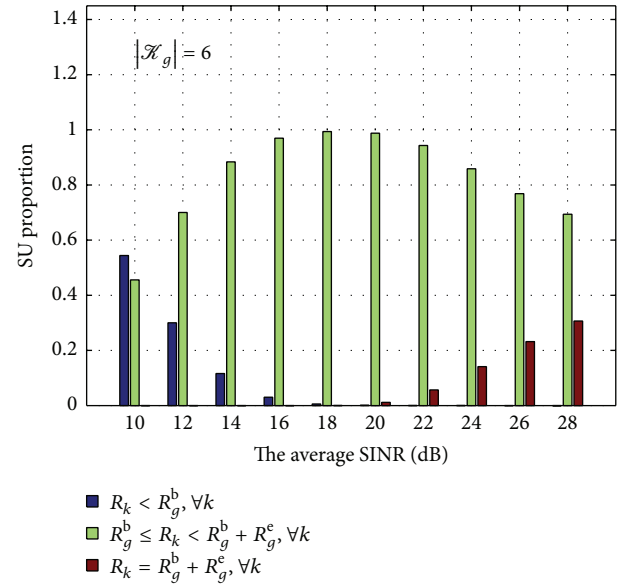

FIGURE 5: The proportion distribution of SUs within three rate ranges.

to the EE optimization thanks to the direct PSNR metric for the video quality. For example, with SINR = 15 dB, when the number of SUs is 4 in each group, the EU optimization can achieve about 120% and 20% performance gain compared to the weighted-PSNR and EE optimizations, respectively. It means that the selection of EU as the optimization objective is much qualified for green video transmission over OFDM-based CR systems.

The proportion distribution is shown in Figure 5 for the SUs, who are classified into three categories according to the total received rate; that is, $R_k < R_g^b$, $R_g^b \le R_k < R_g^b + R_g^e$, and $R_k = R_g^b + R_g^e$, $k \in \mathcal{K}_g$. As the average SINR rises, the proportion of SUs, whose rates are lower than the BL rate, decreases evidently, while the proportion of SUs, who achieve the saturated rate $R_g^b + R_g^e$, increases remarkably. It indicates that the "*bandwidth-hungry*" video services can fully utilize the sensed spectrum by our proposed algorithms. In addition, the proportion (the middle green bars) of the SUs, whose rates satisfy $R_g^b \le R_k < R_g^b + R_g^e$, always dominates the proportion distribution except when the average SINR equals 10 dB, which reveals that the relative fairness among SUs can be ensured as a result of the BL rate requirements and the selected PSNR utility function.

5. Conclusion

This paper studies LVM transmission over OFDM-based CR systems, where multiple interference constraints are necessitated to carry out the performance protection for PUs. An EU-based optimization model, which is well tailored for green video delivery, is formulated, and then the BL and EL spectrum assignments are separately proposed for the complexity reduction. Furthermore, the EU-based power allocation algorithm is also proposed by jointly employing fractional programming and subgradient method. Simulation results show that the proposed power allocation algorithm

can converge to the optimal solution rapidly, and LVM greatly outperforms CM, which is attributed to allowing the elastic data reception. Via the proposed algorithms, the sensed spectrum can be fully exploited by "*bandwidth-hungry*" video services, and the EU-based optimization notably surpasses the EE-based optimization in considering the video quality and energy consumption simultaneously. As the future work, multi-EL modeling and the sequential receiving issue for the video transmission will be considered to further explore the video multicast potential over OFDM-based CR systems.

Appendices

A. Proof of Theorem 1

When the optimal solution is obtained and subcarrier n is assigned to group g, if $p_n = 0$, then $r^{\mathrm{e}}_{g,n} = 0$. Otherwise, if $p_n > 0$, $r^{\mathrm{e}}_{g,n} > 0$, and $r^{\mathrm{e}}_{g,n} \notin \mathscr{B}_n$, then sort the K elements of $\mathscr{B}_n$ in descending order and divide the elements in $\mathscr{B}_n$ into two subsets $\mathscr{B}^-_n, \mathscr{B}^+_n$ according to $r^{\mathrm{e}}_{g,n}$, where $\mathscr{B}^+_n$ is defined as $\{x \mid x \in \mathscr{B}_n, x > r^{\mathrm{e}}_{g,n}\}$ and $\mathscr{B}^-_n = \mathscr{B}_n - \mathscr{B}^+_n$. Actually, the elements of $\mathscr{B}^+_n$ correspond to the achievable rates of SUs who can receive the EL data from subcarrier n. For the optimal solution, $p_n > 0$ requires that $\mathscr{B}^+_n$ must be nonempty, because the empty $\mathscr{B}^+_n$ means $r^{\mathrm{e}}_{g,n}$ is greater than all K achievable rates $r_{m|g,n}$ for $1 \le g \le G, m \in \mathscr{K}_g$, and results in the zero receiving rate on subcarrier n for all SUs.

Supposing that the smallest element in $\mathscr{B}^+_n$ is $r^*_{g,n}$, if $r^*_{g,n}$ is selected as the data transmission rate, then all SUs, who are originally able to receive the data from subcarrier n, can reach a higher receiving rate; that is, $r^{\mathrm{e}}_{g,n} \to r^*_{g,n}$, without harming the receiving rate of other SUs. With the nondecreasing utility functions, the substitution of $r^*_{g,n}$ for $r^{\mathrm{e}}_{g,n}$ will increase the total utility while maintaining the power p_n unchanged. This indicates that the EU can be further improved, which contradicts the optimality assumption. Thus, for $p_n > 0$, $r^{\mathrm{e}}_{g,n}$ must be one of the K achievable rates in $\mathscr{B}_n$.

B. Proof of Theorem 3

The constraints C_1, C_2, and C_3 are linear and thereby convex. In addition, the constraint C_4 can be rewritten as $-\sum_{n\in\Theta^{\mathrm{b}}_g} r_n + R^{\mathrm{b}}_g \le 0$, $1 \le g \le G$. The left-hand side of C_4 is also convex since it is the sum of $-r_n$, which is calculated by a convex function, that is, a negative logarithmic function. The remaining task is to prove that $g(\mathbf{p}, \alpha)$ is convex over the feasible region of p_n, $1 \le n \le N$. To do so, a lemma is introduced as follows.

Lemma B.1. *If a function $g(x)$ is concave, a function $h(x)$ is concave, and the function $\widetilde{h}(x)$ is nondecreasing, then the composition function $f(x) = h(g(x))$ is concave as well.*

In Lemma B.1, with $\mathrm{dom}\, h$ denoting the domain of the function $h(x)$, $\widetilde{h}(x)$ is defined as

$$\widetilde{h}(x) = \begin{cases} h(x) & x \in \mathrm{dom}\, h, \\ -\infty & x \notin \mathrm{dom}\, h. \end{cases} \tag{B.1}$$

The proof can be found in Section 3.2.4 of [26].

Recall the expression of R_k; it is the aggregate rate of all the subcarriers which are occupied by SU k; that is, $R_k = \sum_{n\in\Omega_k} B_0 \log_2(1 + p_n\gamma_n)$. As mentioned above, the rate of each item is a logarithmic function with p_n, and therefore R_k is a concave function with p_n. With $U_k(x)$ being nondecreasing and concave, according to Lemma B.1, $U_k(R_k)$ is concave as well, provided that $\widetilde{U}_k(x)$ is nondecreasing. The additional condition on $\widetilde{U}_k(x)$ can be easily satisfied in practice, due to the fact that the utility function $U_k(x)$ is generally defined over the domain of $\{x \mid x \ge 0\}$, and the nondecreasing feature will be preserved during the extension of $U_k(x)$ to $\widetilde{U}_k(x)$. Thus, $-\alpha U_{\mathrm{total}}(\mathbf{p})$ is convex. In combination with the fact that $E_{\mathrm{total}}(\mathbf{p})$ is linear and convex, $g(\mathbf{p}, \alpha)$ is convex over the feasible region of p_n, $1 \le n \le N$, and consequently problem $\mathscr{OP}_2$ belongs to convex optimization ones.

Conflict of Interests

The authors declare that there is no conflict of interests regarding the publication of this paper.

Acknowledgments

This work is supported by the National Natural Science Foundation of China (61471059), National High-Tech R&D Program (863 Program 2015AA01A705), Fundamental Research Funds for Central Universities (2014ZD03-01), Special Youth Science Foundation of Jiangxi (20133ACB21007), National Key Scientific and Technological Project of China (2013ZX03003012), and Postgraduate Innovation Fund of SICE for BUPT 2015.

References

[1] P. Pirinen, "A brief overview of 5G research activities," in *Proceedings of the 1st IEEE International Conference on 5G for Ubiquitous Connectivity (5GU '14)*, pp. 17–22, IEEE, Äkäslompolo, Finland, November 2014.

[2] E. Hossain and M. Hasan, "5G cellular: key enabling technologies and research challenges," *IEEE Instrumentation & Measurement Magazine*, vol. 18, no. 3, pp. 11–21, 2015.

[3] A. Osseiran, F. Boccardi, V. Braun et al., "Scenarios for 5G mobile and wireless communications: the vision of the METIS project," *IEEE Communications Magazine*, vol. 52, no. 5, pp. 26–35, 2014.

[4] J. Mitola and G. Q. Maguire Jr., "Cognitive radio: making software radios more personal," *IEEE Personal Communications*, vol. 6, no. 4, pp. 13–18, 1999.

[5] Y.-C. Liang, K.-C. Chen, G. Y. Li, and P. Mähönen, "Cognitive radio networking and communications: an overview," *IEEE Transactions on Vehicular Technology*, vol. 60, no. 7, pp. 3386–3407, 2011.

[6] S. Chen and J. Zhao, "The requirements, challenges, and technologies for 5G of terrestrial mobile telecommunication," *IEEE Communications Magazine*, vol. 52, no. 5, pp. 36–43, 2014.

[7] Y. Gao, W. Xu, K. Yang, K. Niu, and J. Lin, "Energy-efficient transmission with cooperative spectrum sensing in cognitive radio networks," in *Proceedings of the IEEE Wireless Communications and Networking Conference (WCNC '13)*, pp. 7–12, Shanghai, China, April 2013.

[8] T. Zhang and D. H. Tsang, "Cooperative sensing scheduling for energy-efficient cognitive radio networks," *IEEE Transactions on Vehicular Technology*, vol. 64, no. 6, pp. 2648–2662, 2015.

[9] Y. Wang, W. Xu, K. Yang, and J. Lin, "Optimal energy-efficient power allocation for OFDM-based cognitive radio networks," *IEEE Communications Letters*, vol. 16, no. 9, pp. 1420–1423, 2012.

[10] J. Mao, G. Xie, J. Gao, and Y. Liu, "Energy efficiency optimization for ofdm-based cognitive radio systems: a water-filling factor aided search method," *IEEE Transactions on Wireless Communications*, vol. 12, no. 5, pp. 2366–2375, 2013.

[11] S. Wang, M. Ge, and W. Zhao, "Energy-efficient resource allocation for OFDM-based cognitive radio networks," *IEEE Transactions on Communications*, vol. 61, no. 8, pp. 3181–3191, 2013.

[12] S. Wang, W. Shi, and C. Wang, "Energy-efficient resource management in OFDM-based cognitive radio networks under channel uncertainty," *IEEE Transactions on Communications*, vol. 63, no. 9, pp. 3092–3102, 2015.

[13] R. O. Afolabi, A. Dadlani, and K. Kim, "Multicast scheduling and resource allocation algorithms for OFDMA-based systems: a survey," *IEEE Communications Surveys and Tutorials*, vol. 15, no. 1, pp. 240–254, 2013.

[14] N. Rupasinghe and I. Guvenc, "Licensed-assisted access for WiFi-LTE coexistence in the unlicensed spectrum," in *Proceedings of the IEEE Globecom Workshops (GC Wkshps '14)*, pp. 894–899, Austin, Tex, USA, December 2014.

[15] D. T. Ngo, C. Tellambura, and H. H. Nguyen, "Resource allocation for OFDMA-based cognitive radio multicast networks with primary user activity consideration," *IEEE Transactions on Vehicular Technology*, vol. 59, no. 4, pp. 1668–1679, 2010.

[16] K. Yang, W. Xu, S. Li, and J. Lin, "A distributed multiple description coding multicast resource allocation scheme in OFDM-based cognitive radio networks," in *Proceedings of the IEEE Wireless Communications and Networking Conference (WCNC '13)*, pp. 210–215, IEEE, Shanghai, China, April 2013.

[17] K. Yang, W. Xu, S. Li, J. Lin, and W. Wu, "A statistical-CSI-based scheme for multiple description coding multicast in CRNs," *IEEE Signal Processing Letters*, vol. 21, no. 2, pp. 213–216, 2014.

[18] H. Zhang, Y. Zheng, M. A. Khojastepour, and S. Rangarajan, "Cross-layer optimization for streaming scalable video over fading wireless networks," *IEEE Journal on Selected Areas in Communications*, vol. 28, no. 3, pp. 344–353, 2010.

[19] D. Hu, S. Mao, Y. T. Hou, and J. H. Reed, "Scalable video multicast in cognitive radio networks," *IEEE Journal on Selected Areas in Communications*, vol. 28, no. 3, pp. 434–444, 2010.

[20] T. Weiss, J. Hillenbrand, A. Krohn, and F. K. Jondral, "Mutual interference in OFDM-based spectrum pooling systems," in *Proceedings of the IEEE 59th Vehicular Technology Conference. VTC 2004-Spring*, vol. 4, pp. 1873–1877, IEEE, May 2004.

[21] H. Schwarz, D. Marpe, and T. Wiegand, "Overview of the scalable video coding extension of the H.264/AVC standard," *IEEE Transactions on Circuits and Systems for Video Technology*, vol. 17, no. 9, pp. 1103–1120, 2007.

[22] H. M. Radha, M. Van der Schaar, and Y. Chen, "The MPEG-4 fine-grained scalable video coding method for multimedia streaming over IP," *IEEE Transactions on Multimedia*, vol. 3, no. 1, pp. 53–68, 2001.

[23] Z. Shen, J. G. Andrews, and B. L. Evans, "Adaptive resource allocation in multiuser OFDM systems with proportional rate constraints," *IEEE Transactions on Wireless Communications*, vol. 4, no. 6, pp. 2726–2737, 2005.

[24] G. Bansal, M. J. Hossain, and V. K. Bhargava, "Adaptive power loading for OFDM-based cognitive radio systems with statistical interference constraint," *IEEE Transactions on Wireless Communications*, vol. 10, no. 9, pp. 2786–2791, 2011.

[25] W. Dinkelbach, "On nonlinear fractional programming," *Management Science*, vol. 13, no. 7, pp. 492–498, 1967.

[26] S. Boyd and L. Vandenberghe, *Convex Optimization*, Cambridge University Press, 2004.

[27] D. P. Bertsekas, *Nonlinear Programming*, Athena Scientific, 1999.